Report

Cell Reports

A Role for IFITM Proteins in Restriction of *Mycobacterium tuberculosis* Infection

Graphical Abstract

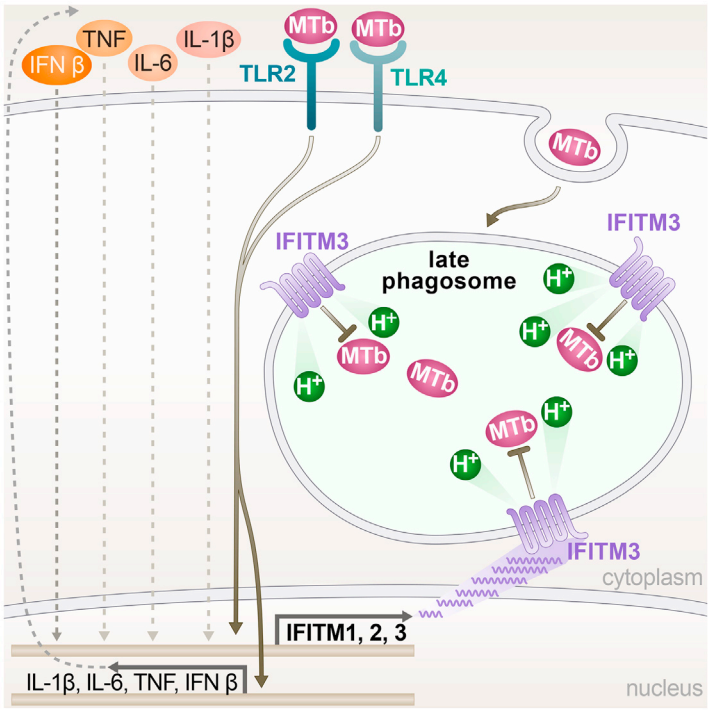

Highlights

- *Mycobacterium tuberculosis* (MTb) and TLR2/4 signaling induce *IFITM1–3* transcription
- IFITM1–3 restrict intracellular growth of MTb
- IFITM3 co-localizes with MTb, especially in late phagosomes
- IFITM3 enhances intracellular endosomal acidification in MTb-infected cells

Authors

Shahin Ranjbar, Viraga Haridas, Luke D. Jasenosky, James V. Falvo, Anne E. Goldfeld

Correspondence

shahin.ranjbar@childrens.harvard.edu (S.R.),
anne.goldfeld@childrens.harvard.edu (A.E.G.)

In Brief

Ranjbar et al. find that IFITM family members 1–3, which restrict infection by a wide range of viruses, inhibit a bacterial pathogen, *Mycobacterium tuberculosis* (MTb). MTb infection, signaling via TLR2 and TLR4, and MTb-induced cytokines all induce *IFITM1–IFITM3* gene transcription. IFITM3, which has the greatest anti-MTb activity, associates with and increases acidification of MTb phagosomes.

Ranjbar et al., 2015, Cell Reports *13*, 874–883
November 3, 2015 ©2015 The Authors
http://dx.doi.org/10.1016/j.celrep.2015.09.048

OPEN ACCESS
CellPress

Cell Reports
Report

A Role for IFITM Proteins in Restriction of *Mycobacterium tuberculosis* Infection

Shahin Ranjbar,[1,*] Viraga Haridas,[1] Luke D. Jasenosky,[1] James V. Falvo,[1] and Anne E. Goldfeld[1,*]
[1]Program in Cellular and Molecular Medicine, Children's Hospital Boston, Boston, MA 02115, USA
*Correspondence: shahin.ranjbar@childrens.harvard.edu (S.R.), anne.goldfeld@childrens.harvard.edu (A.E.G.)
http://dx.doi.org/10.1016/j.celrep.2015.09.048

SUMMARY

The interferon (IFN)-induced transmembrane (IFITM) proteins are critical mediators of the host antiviral response. Here, we expand the role of IFITM proteins to host defense against intracellular bacterial infection by demonstrating that they restrict *Mycobacterium tuberculosis* (MTb) intracellular growth. Simultaneous knockdown of IFITM1, IFITM2, and IFITM3 by RNAi significantly enhances MTb growth in human monocytic and alveolar/epithelial cells, whereas individual overexpression of each IFITM impairs MTb growth in these cell types. Furthermore, MTb infection, Toll-like receptor 2 and 4 ligands, and several proinflammatory cytokines induce *IFITM1–3* gene expression in human myeloid cells. We find that IFITM3 co-localizes with early and, in particular, late MTb phagosomes, and overexpression of IFITM3 enhances endosomal acidification in MTb-infected monocytic cells. These findings provide evidence that the antiviral IFITMs participate in the restriction of mycobacterial growth, and they implicate IFITM-mediated endosomal maturation in its antimycobacterial activity.

INTRODUCTION

Successful intracellular pathogens often use strategies to gain access to cellular compartments required for their survival ahead of the initiation of innate host antimicrobial mechanisms. The well-characterized interferon (IFN)-induced transmembrane (*IFITM*) gene family encodes highly conserved proteins that act at early steps post-viral entry, thereby precluding establishment of productive infection (Diamond and Farzan, 2013). In humans, three IFITMs (IFITM1, IFITM2, and IFITM3) are widely expressed, and the genes encoding these restriction factors are activated by types I and II IFN stimulation via IFN-sensitive response elements (ISREs) in their regulatory regions (Ackrill et al., 1991; Friedman et al., 1984; Kelly et al., 1985; Lewin et al., 1991; Reid et al., 1989). While IFITM1–3 share substantial sequence similarity, IFITM1 primarily is found at the cell periphery due to its lack of an N-terminal 21 amino acid sequence that promotes IFITM2 and IFITM3 recruitment to late endosomal/lysosomal membranes (Jia et al., 2012; John et al., 2013; Weston et al., 2014).

Virus restriction by individual IFITMs depends both on cell type and the intracellular location of each family member. For example, HIV, which undergoes viral envelope-cell membrane fusion at the cell surface or within early endosomes, is more restricted by IFITM1 (Lu et al., 2011), while influenza A virus, which requires pH-dependent changes in envelope glycoprotein conformation for viral fusion at late endosomes/lysosomes, is more restricted by IFITM2/3 (Brass et al., 2009; Desai et al., 2014; Feeley et al., 2011; John et al., 2013). IFITMs appear to block viral infection by reducing host membrane fluidity at sites of viral fusion through self-interactions and/or interactions with nearby transmembrane proteins, leading to inhibition of viral fusion pore formation and increased trafficking of trapped viruses to the lysosome for degradation (Desai et al., 2014; Lin et al., 2013).

Evasion of lysosomal targeting is a survival strategy not only for viruses, but also is employed by many intracellular bacteria, including *Mycobacterium tuberculosis* (MTb). Virulent MTb employs several mechanisms to prevent acidification of the phagosome, thereby supporting its own survival (Stanley and Cox, 2013). For example, the vacuolar ATPase (v-ATPase), which is a primary mediator of endosomal acidification, is excluded from the MTb-containing phagosome by MTb's bacterial tyrosine phosphatase (Bach et al., 2008; Sturgill-Koszycki et al., 1994; Wong et al., 2011). Intriguingly, IFITM3 was found to co-immunoprecipitate with a subunit of the v-ATPase (Wee et al., 2012). Furthermore, overexpression of IFITM3 has been shown to increase endosomal pH and expand the size and number of intracellular acidic compartments (Feeley et al., 2011; Mudhasani et al., 2013; Wee et al., 2012).

Here, we show that *IFITM1*, *IFITM2*, and *IFITM3* are transcriptionally activated in response to MTb infection and by several proinflammatory cytokines produced during MTb infection. Strikingly, depletion of these IFITMs significantly enhances MTb growth in human monocytes. Furthermore, IFITM3 co-localizes with the maturing MTb phagosome and its overexpression significantly restricts MTb growth and enhances endosomal acidification in MTb-infected cells. These findings provide evidence that IFITM family members directly inhibit a bacterial pathogen.

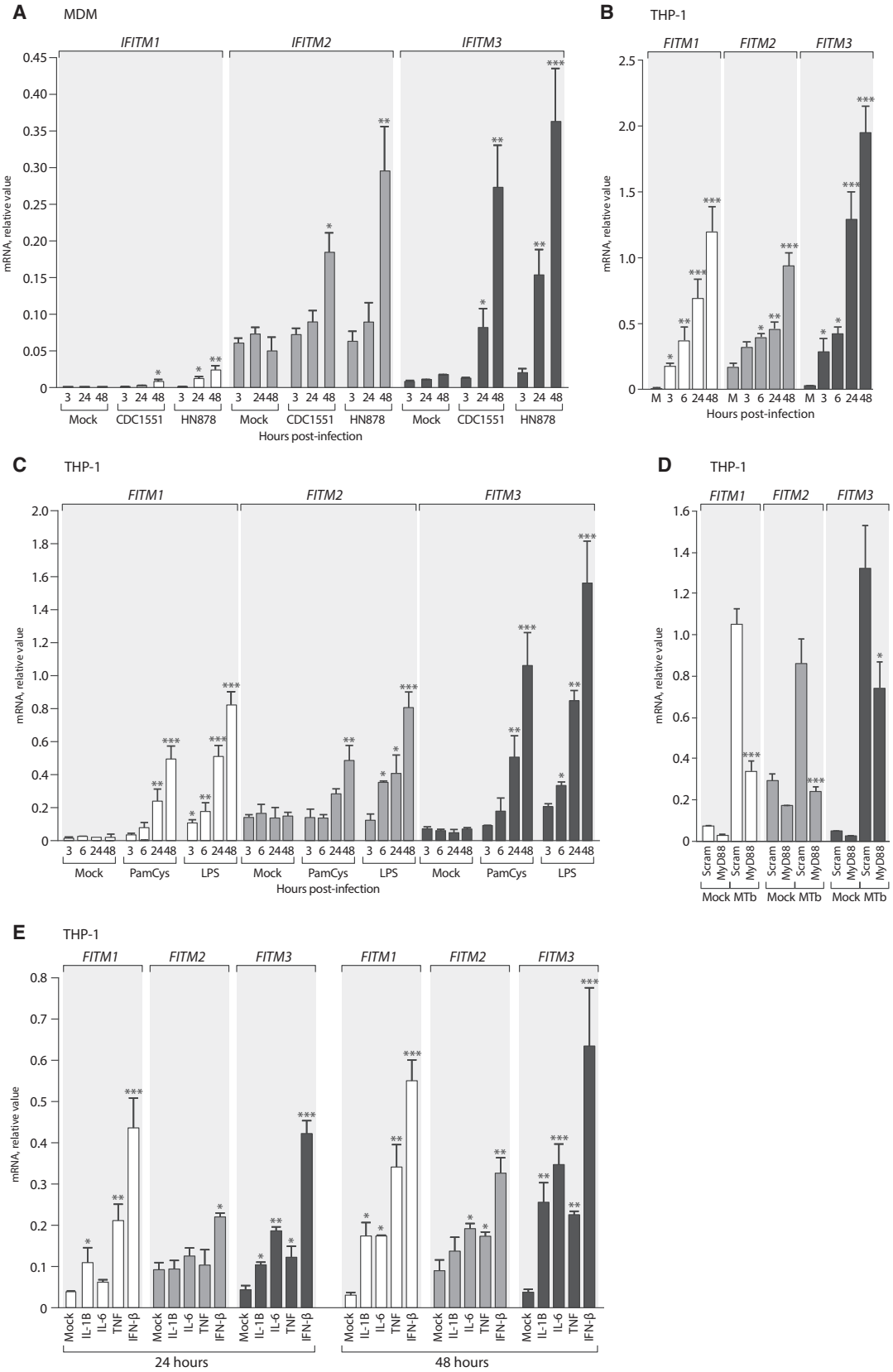

(legend on next page)

RESULTS

MTb Infection and TLR2/4-, MyD88-, and Cytokine-Signaling Pathways Promote Expression of IFITM1, 2, and 3 mRNA

To determine whether MTb infection induces transcriptional activation of the *IFITM*s, we infected primary human monocyte-derived macrophages (MDMs) with the clinical MTb strains CDC1551 and HN878 and measured *IFITM1–3* mRNA levels at 3, 24, and 48 hr post-infection. All three genes were significantly induced by CDC1551 and HN878 (Figure 1A) in MDMs, and a similar response was seen at 6, 24, and 48 hr in H37Rv-MTb-infected THP-1 monocytes (Figure 1B).

MTb triggers signaling by the pattern recognition receptors (PRRs) Toll-like receptor (TLR)2 and TLR4, leading to the activation of innate immune response genes (Means et al., 1999; Underhill et al., 1999; reviewed in Falvo et al., 2011). As shown in Figure 1C, activation of THP-1 cells with the TLR2 agonist Pam3Cys or with the TLR4 agonist lipopolysaccharide (LPS) significantly induced *IFITM1–3* gene expression, which reached levels comparable to what was seen with live MTb infection by 48 hr post-stimulation.

Upon engagement of TLR2 or TLR4, the adaptor molecule MyD88 transmits signals to downstream kinases, including IRAK1 and TRAF6, which mediate activation of the MAPK and NF-κB pathways and innate immune gene synthesis (Deguine and Barton, 2014; Falvo et al., 2011). As shown in Figure 1D, when MyD88 expression was depleted in THP-1 cells by small hairpin RNA (shRNA), MTb-induced *IFITM1–3* mRNA synthesis was impaired significantly, indicating that this signaling adaptor participates in *IFITM* gene induction by MTb. We obtained similar results in THP-1 cells in which IRAK1 or TRAF6 expression was ablated (Figure S1), indicating that TLR-mediated MyD88 signaling directly leads to *IFITM* transcription.

Although MTb induces the expression of type I IFN (Berry et al., 2013), the prototypical stimulus of *IFITM* gene expression, MTb also induces the expression of other proinflammatory cytokines that are critical mediators of the host innate immune response, including IL-1β, IL-6, and TNF (Etna et al., 2014). Direct activation of the MTb-responsive PRRs TLR2 and TLR4 on THP-1 cells led to significantly enhanced levels of IL-1β, TNF, and IL-6 mRNA by 24 hr (Figure S2). While IL-1β signaling requires the MyD88/IRAK1/TRAF6 axis, TNF and IL-6 activate distinct signaling pathways (Falvo et al., 2011). To investigate if these cytokines directly induce *IFITM* gene expression in monocytic cells, we treated THP-1 cells with recombinant IL-1β, IL-6, or TNF, or, as a positive control, recombinant IFN-β, and assessed *IFITM1–3* transcript levels. As anticipated, IFN-β stimulation dramatically induced IFITM1–3 transcription (Figure 1E). By 24 hr post-stimulation, both IL-1β and TNF also significantly upregulated *IFITM1* gene expression, and all three cytokines significantly increased *IFITM3* mRNA levels. At 48 hr, IFITM1 mRNA synthesis also was increased significantly by IL-6, and *IFITM2* transcription was enhanced significantly at this time point by both IL-6 and TNF (Figure 1E). Taken together, these data indicate that *IFITM1–3* gene expression is induced by secondary signaling pathways, including those triggered by binding of IL-1β, IL-6, and TNF to their cognate receptors, activated during MTb infection in addition to being directly activated by MTb and MyD88-dependent TLR ligation.

Knockdown of IFITM1–3 Expression Enhances Intracellular Growth of MTb in Monocytes

To directly assess the role of IFITM proteins in MTb infection, we stably transduced THP-1 cells with a lentiviral vector encoding an shRNA targeting a conserved region present in *IFITM1*, *2*, and *3* mRNAs. We infected these cells with mCherry-expressing MTb (H37Rv-mCherry), after demonstrating that expression of each IFITM was ablated by >80% (Figure 2A). As shown in a representative flow cytometry assay in Figure 2B, after 24 hr, control cells were 29.8% infected as compared to IFITM1–3 knockdown (KD) THP-1 cells, which were 51.8% infected. At 48 hr post-infection, control cells were 38.4% infected and IFITM1–3 KD cells were 65% infected.

When we used colony-forming unit (CFU) assay to measure bacterial growth, significant increases ($p < 0.01$) in MTb growth were observed at 2 and 3 days post-infection in IFITM-KD versus control THP-1 cells (Figure 2C), confirming the flow cytometry data we obtained. Furthermore, bacterial uptake was similar in both the IFITM-KD and control THP-1 cells (Figure 2C), indicating that the IFITMs restrict MTb at a post-entry stage in human monocytes.

Overexpression of IFITM1, 2, or 3 Restricts MTb Infection in Monocytes

To investigate the relative impact of each IFITM family member on MTb growth in monocytes, we next overexpressed IFITM1, IFITM2, or IFITM3 in THP-1 cells by lentiviral transduction (Figure S3). At 24 hr post-infection, H37Rv-mCherry signal was lower in each IFITM-overexpressing cell line compared to cells transduced with an empty lentiviral vector (Figure 3A). As shown in Figure 3A, IFITM3 overexpression led to the greatest decrease in MTb growth (38.5% compared to 26.7% for IFITM1 and 24.7% for IFITM2).

Figure 1. *IFITM1*, *IFITM2*, and *IFITM3* Gene Expression Is Induced in Human Macrophages and Monocytic Cells in Response to MTb Infection via TLR2/4- and MyD88-Dependent Signaling Pathways

(A) MDMs were left uninfected (mock) or infected with MTb strains CDC1551 or HN878 as indicated for 3, 24, and 48 hr and *IFITM1–3* transcripts were measured.

(B) THP-1 cells were left uninfected (mock) or infected with MTb strain H37Rv for 3, 6, 24, and 48 hr and *IFITM1–3* transcripts were measured.

(C) THP-1 cells were left untreated (mock) or treated with the TLR2 agonist Pam3Cys (100 ng/ml) or the TLR4 agonist LPS (100 ng/ml) for 3, 6, 24, and 48 hr and *IFITM1–3* transcripts were measured.

(D) THP-1 cells in which MyD88 is constitutively ablated by shRNA, or THP-1 cells expressing a control shRNA, were infected with MTb strain H37Rv or left uninfected (mock) for 48 hr and *IFITM1–3* transcripts were measured.

(E) THP-1 cells were left untreated (mock) or treated with recombinant IL-1β (100 ng/ml), IL-6 (50 ng/ml), TNF (10 ng/ml), or IFN-β (100 ng/ml) for 24 and 48 hr. *IFITM1–3* and cyclophilin B mRNA levels were assayed using qPCR. Results are the mean ± SEM from three independent experiments (*$p \leq 0.05$, **$p \leq 0.01$, ***$p \leq 0.005$).

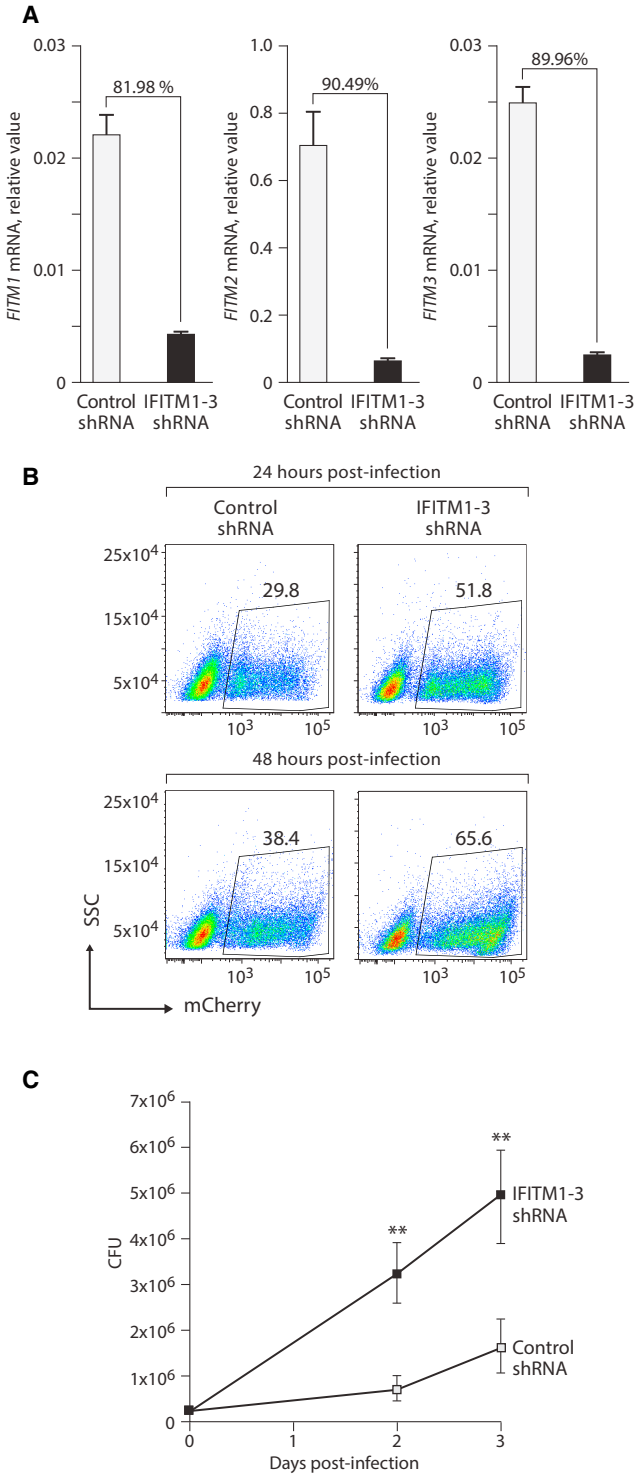

Figure 2. Ablation of Endogenous IFITM1–3 Increases MTb Replication

(A) *IFITM1*, *IFITM2*, and *IFITM3* mRNA levels were measured in THP-1 transduced with a lentiviral vector encoding a single shRNA targeting IFITM1, 2, and 3, or a vector encoding a control shRNA.

(B) IFITM1–3 shRNA KD or control THP-1 cells were infected with MTb strain H37Rv-mCherry for 24 or 48 hr and analyzed by flow cytometry. Gated area and numerical values show the percentage of the cells infected with bacilli. Dot plots are representative of three independent experiments.

(C) CFU assay of IFITM-KD or control THP-1 cells at days 0, 2, and 3 post-infection with H37Rv-mCherry. Results are the mean ± SEM from two experiments (**p < 0.01).

To quantitatively measure the impact of IFITM3 overexpression on H37Rv-mCherry infection, we utilized ImageStream technology, which allowed us to capture images of individual cells containing intracellular MTb. After eliminating cells from the analysis that exhibited H37Rv-mCherry surface attachment (Figures 3B and 3C; Figure S4), we used IDEAS software to measure mCherry pixel intensity in IFITM3-overexpressing and control cells. There was a significant decrease in mean per-cell mCherry intensity in the IFITM3-overexpressing THP-1 cells ($p = 0.007$) (Figure 3B). By contrast, there was a significant increase in mean per-cell mCherry intensity in the IFITM-KD versus control THP-1 cells ($p < 0.0001$) (Figure 3C), consistent with the fluorescence-activated cell sorting (FACS) and CFU data, further supporting a role for the IFITMs—and IFITM3 in particular—in restriction of MTb growth.

Intracellular Localization of IFITM3 Overlaps with MTb Bacilli in Early and Late Phagosomes

IFITM3's antiviral activity has been associated with its distribution to late endosomal/lysosomal membranes and its ability to promote increases in the number and size of acidic intracellular compartments (Feeley et al., 2011; Mudhasani et al., 2013; Wee et al., 2012). To determine if a similar mechanism was involved in IFITM3's modulation of MTb infection, we investigated the association of IFITM3 and MTb with endosomal compartments in A549 human lung alveolar carcinoma cells. A549 cells transcribe *IFITM1–3* in response to IFN-β stimulation (Figure S5) and are a long-standing model for MTb infection of the airway epithelium (Bermudez and Goodman, 1996; McDonough and Kress, 1995), and they have been used extensively to examine IFITM antiviral activity (Brass et al., 2009; Huang et al., 2011; John et al., 2013). Furthermore, as we found in THP-1 cells, shRNA-mediated depletion of the IFITMs in A549 cells led to greater MTb growth at 24 (57%) and 48 (30%) hr post-infection (Figure S6), and overexpression of IFITM1, 2, or 3 in A549 cells inhibited MTb growth, with IFITM3 exhibiting the strongest effect (Figures S6C and S6D), supporting the relevance of A549 cells for examination of IFITM3-MTb intracellular association by confocal microscopy.

Next, we introduced a C-terminal V5-tagged version of IFITM3 into A549 cells to investigate changes in intracellular IFITM3 distribution during MTb infection. Like endogenous IFITM3, C-terminal epitope-tagged IFITM3 localizes mainly to late endosomes/lysosome in A549 cells (Amini-Bavil-Olyaee et al., 2013; Feeley et al., 2011; Huang et al., 2011; Williams et al., 2014). After infection of IFITM3-V5 or control A549 cells, H37Rv-mCherry bacilli co-localized with IFITM3 at $Rab5^+$ phagosomal compartments (Figure 4A, top and graph; $p < 0.01$) and, to a relatively greater degree, at late $Rab7^+$ phagosomal compartments (Figure 4A, bottom and graph; $p < 0.005$), indicating that IFITM3 associates with MTb phagosomes that are likely progressing to phagolysosomal maturation. We note that IFITM3 overexpression

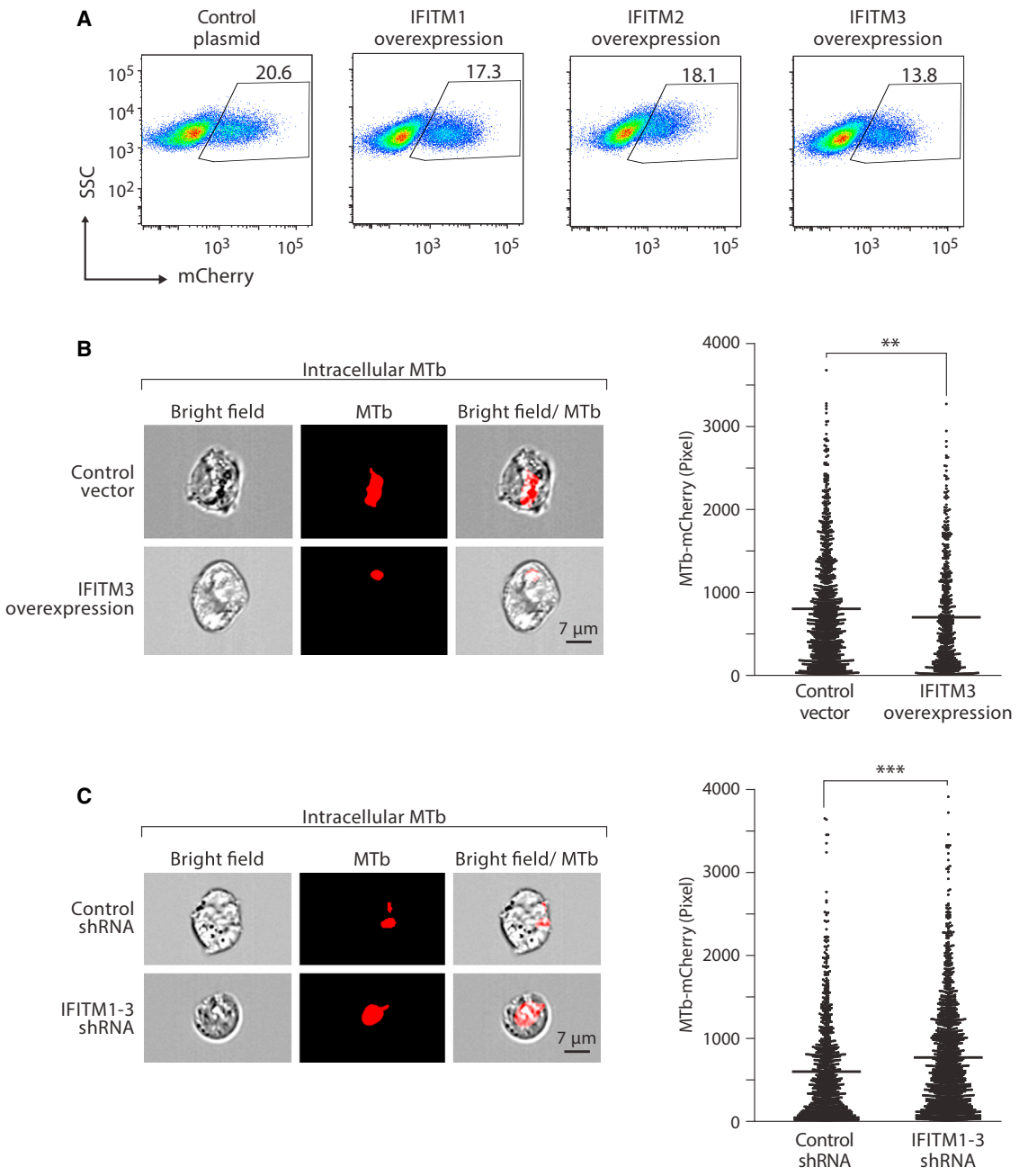

Figure 3. IFITM1, IFITM2, or IFITM3 Overexpression Inhibits MTb Replication in Monocytic Cells

(A) THP-1 cells transduced with an empty control vector or vectors encoding *IFITM1*, *IFITM2*, or *IFITM3* were infected with MTb H37Rv-mCherry for 24 hr. Gated area and numerical values show the percentage of the cells infected with bacilli. Dot plots are representative of three independent experiments.

(B and C) Representative images of intracellular mycobacteria that are associated with individual cells indicated after acquisition on an ImageStream X Mark II instrument and IDEAS software analysis. Bright-field microscopy indicates cells magnified 60× and infected with MTb H37Rv-mCherry for 24 hr. THP-1 cells were transduced with (B) control or IFITM3 overexpression vectors or (C) vectors encoding IFITM1–3 shRNA or control shRNA. Images shown from left to right are as follows: bright field (gray) indicating cellular outline, MTb-mCherry fluorescence (red) indicating MTb, and merged image of MTb-mCherry fluorescence and bright field showing intracellular MTb. Dot plot graphs on the right-hand side show the pixel intensity of intracellular mCherry in the infected cells. Results are from one of two independent experiments, acquiring 2,500 cells per sample each time (**$p < 0.01$, ***$p < 0.005$).

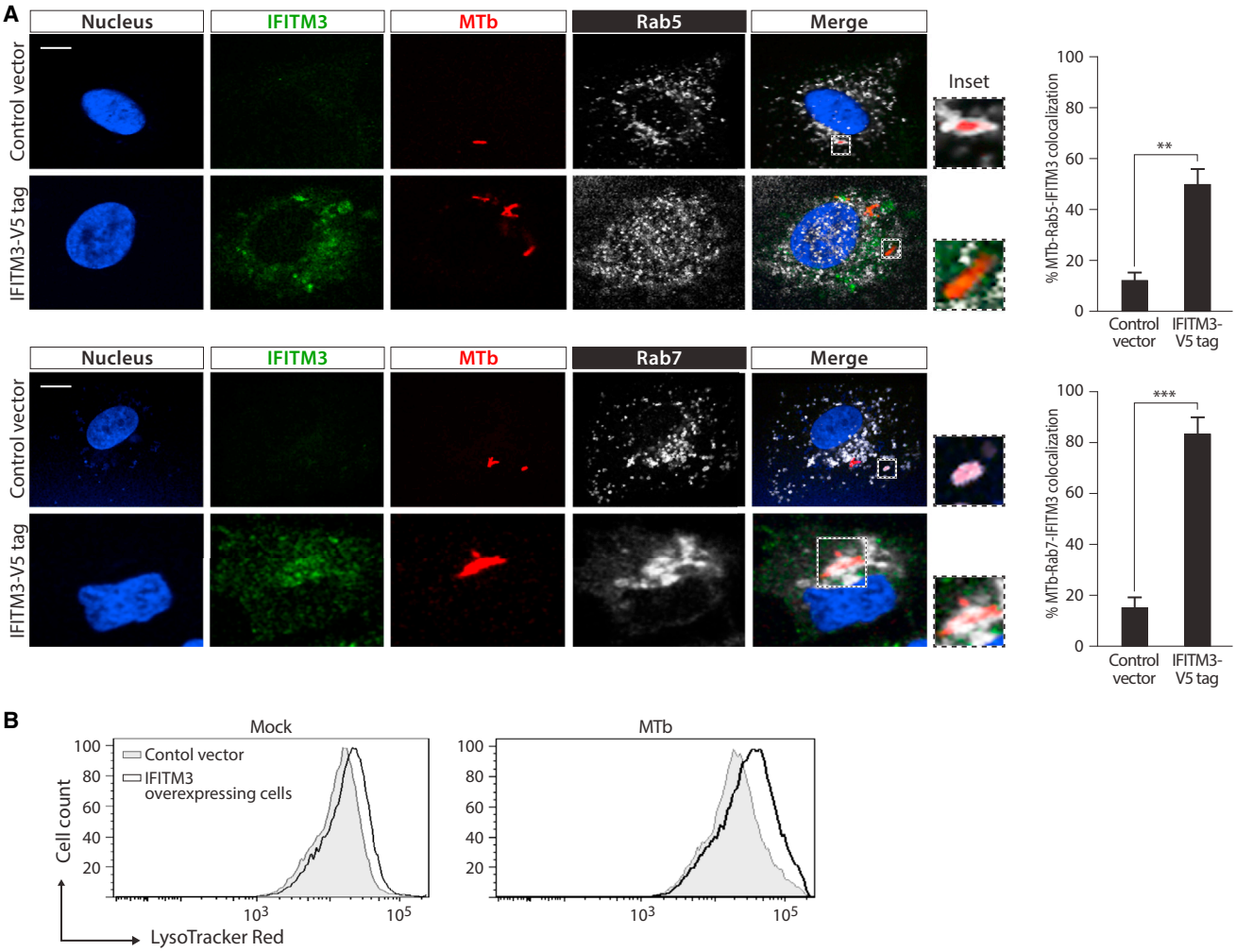

Figure 4. IFITM3 Co-localizes with MTb as Phagosome Maturation Proceeds and IFITM3 Overexpression Enhances Endosomal Acidification in the Presence of MTb Infection

(A) A549 cells transduced with IFITM3-V5 tag (IFITM3) or control vectors were infected with MTb H37Rv-mCherry as described in the Experimental Procedures. (Top) MTb-mCherry- (red) infected cells were immunostained with anti-V5 (IFITM3, green), anti-Rab5 (white), and DAPI (nuclei, blue). The graph shows quantitative measurement of MTb co-localization with IFITM3 and Rab5. (Bottom) MTb-mCherry- (red) infected cells were immunostained with anti-V5 (IFITM3, green), anti-Rab7 (white), and DAPI (nuclei, blue). The graph shows quantitative measurement of MTb co-localization with IFITM3 and Rab7. Scale bar, 10 μM. Enlarged images on the right-hand side of the merged images show the MTb-containing phagosomes. Data are representative of four independent experiments. Results are the mean ± SEM (**$p < 0.01$, ***$p < 0.005$).

(B) THP-1 cells transduced with a control vector or a vector overexpressing IFITM3 were left uninfected (mock) or infected with MTb H37Rv for 48 hr, after which they were incubated with LysoTracker Red for 2 hr. Histograms show LysoTracker Red signal in the control and IFITM3-overexpressing cells in the absence (left) or presence (right) of MTb infection.

increased the staining intensity of Rab7 (Figure 4, bottom), consistent with previous observations (Feeley et al., 2011).

IFITM3 Overexpression Enhances Intracellular Endosomal Acidification in MTb-Infected Cells

To determine whether IFITM3 overexpression can augment endosomal acidity in the context of virulent MTb infection, we next infected IFITM3-overexpressing or control THP-1 cells with H37Rv-MTb and stained them with LysoTracker Red, a fluorescent indicator of acidic intracellular organelles. Levels of endosomal acidification were higher in IFITM3-overexpressing versus control THP-1 cells, and this was maintained and even enhanced in the presence of MTb infection (Figure 4B). These results indicate that endosomal acidification mediated by MTb may be one mechanism underlying its antimycobacterial activity.

DISCUSSION

Our findings expand the role of a well-established family of antiviral restriction factors to control of a major bacterial pathogen. In a previous study, no difference was found in lung bacterial

load between wild-type and *Ifitm3*$^{-/-}$ C57BL/6 mice at 30 days post-aerosol infection with H37Rv-MTb (Everitt et al., 2013). However, only early time points (<30 days) post-infection were evaluated in this study, and it is clear that many immunological factors important for TB control become evident only at later stages in mice (Mayer-Barber and Sher, 2015). We previously demonstrated, for example, that MTb lung burden is equivalent at 6 weeks post-infection in wild-type mice and mice deficient in the transcription factor NFATp, but the NFATp$^{-/-}$ mice succumbed more rapidly (median 119 versus 205 days) and lung bacterial burden was 10^3 higher in these mice at the time of death/sacrifice (Via et al., 2012). In another example, MTb lung burden was higher in IL-6-deficient versus wild-type mice early after infection, but the IL-6$^{-/-}$ mice contained bacterial growth at later time points (Saunders et al., 2000). Moreover, while three *IFITM*s have been identified in humans, mice possess four *Ifitm* genes (Sällman Almén et al., 2012; Zhang et al., 2012), suggesting that redundancy among the IFITMs may have precluded clear identification of a phenotype. Finally, although the murine TB model has proved valuable for the elucidation of immunoregulatory pathways involved in TB control that also are critical in humans, inflammatory responses in mice, particularly at the level of monocyte/macrophage function and TLR activation, are imperfect representatives of what occurs in humans (Seok et al., 2013), and the challenge strain used by Everitt et al. (2013), H37Rv, is less virulent than clinical strains (Palanisamy et al., 2009; Park et al., 2006). Thus, the study of TB in *Ifitm3*$^{-/-}$ C57BL/6 mice (Everitt et al., 2013) does not rule out a role for IFITM3, or the IFITM family, in the innate immune response to TB.

Intriguingly, a SNP in the *IFITM3* promoter (rs3888188; T > G), which reduces transcriptional activation of *IFITM3*, has been associated with increased susceptibility to TB in Han Chinese children (Shen et al., 2013). A C to T SNP in the *IFITM3* cDNA, which was speculated to disrupt a splice-acceptor site and produce an N-terminal truncated version of the protein, has been associated with increased severity of influenza virus infection and accelerated HIV disease (Everitt et al., 2012; Zhang et al., 2013, 2015), although the impact of this SNP on influenza morbidity/mortality in humans (Mills et al., 2014) and the importance of N-terminal truncation of IFITM3 on the restriction of influenza virus infection (Williams et al., 2014) are still points of debate. It is of interest to determine if these or other SNPs in the genes encoding IFITM1–3 are associated with TB susceptibility in other patient populations.

Our data demonstrate that MTb infection induces *IFITM* gene expression. Previously, it was reported that LPS induces *IFITM1* mRNA synthesis in human dendritic cells (Ishii et al., 2005); *Ifitm1* and murine-specific *Ifitm6* transcription in RAW264.7 macrophages (Han et al., 2011); and *Ifitm3* gene expression in murine astrocytes, a process that was dependent on autocrine IFNβ signaling (Nakajima et al., 2014). We found that MyD88 KD reduces MTb-induced *IFITM1–3* mRNA levels, demonstrating a direct role for TLRs and MyD88-dependent autocrine/paracrine factors, such as IL-1β, in activation of these genes. Indeed, we found that IL-1β also induces *IFITM1–3* transcription in human monocytes, extending previous findings that IL-1β activates *IFITM3* mRNA synthesis in hepatocarcinoma cells and murine astrocytes (Nakajima et al., 2014). As TNF and IL-6 also induced the transcription of *IFITM1–3* in monocytes, it is likely that soluble factors produced during MTb infection further amplify PRR-driven *IFITM1–3* mRNA levels. The cytosolic DNA sensor cyclic GMP-AMP synthase (cGAS), which recently has been shown to trigger type I IFN synthesis in MTb-infected cells (Collins et al., 2015; Dey et al., 2015; Wassermann et al., 2015; Watson et al., 2015), also may play a role in MTb-induced *IFITM* synthesis.

Arrest of phagosome maturation is a hallmark of virulent MTb infection (Armstrong and Hart, 1971). A mechanism of MTb-mediated phagosome arrest is the exclusion of the host v-ATPase from the phagosomal membrane (Sturgill-Koszycki et al., 1994; Wong et al., 2011). Notably, IFITM3 overexpression leads to an increase in the size and number of acidic compartments in murine and human cells (Feeley et al., 2011; Mudhasani et al., 2013; Wee et al., 2012), and IFITM3 interacts with v-ATPase and potentially stabilizes its association with endosomal membranes (Wee et al., 2012). Our findings that IFITM3 co-localizes with the MTb phagosome and that increased IFITM3-mediated intracellular acidity is maintained even in the presence of MTb infection suggest that IFITM3 (and potentially IFITM1/2) impedes productive MTb infection in a manner similar to its antiviral role. Because several other pathogenic intracellular bacteria, including *Salmonella enterica* and *Yersinia pestis*, also depend on phagosomal maturation arrest for survival and growth (Smith and May, 2013), it is possible that the IFITMs may contribute to host control of a diverse range of bacterial pathogens.

MTb appears to have emerged from Africa with the first humans (Gagneux, 2012). As gene duplication events have led to diverse numbers of *IFITM* genes in the primate lineage (Zhang et al., 2012), it is intriguing to speculate that the *IFITM* genes have co-evolved with mycobacteria as well as viral pathogens and have contributed to the constantly co-evolving host-pathogen dynamic driven by TB disease in humans.

EXPERIMENTAL PROCEDURES

Ethics Statement

For isolation of peripheral blood mononuclear cells (PBMCs), we obtained unidentified, discarded leukocyte collars from the Boston Children's Hospital Blood Donor Center.

MTb Culture

The MTb strains H37Rv, H37Rv-mCherry (kindly provided by Dr. Sarah Fortune; Sillé et al., 2011), HN878, and CDC1551 were prepared as described before (Ranjbar et al., 2009). Cultures were grown to an OD_{650} of 0.4 at 37°C to ensure they were logarithmic growth phase, and bacteria were pelleted, washed, resuspended in PBS, and passed through a 5-μM filter to ensure single-cell suspension. Bacterial numbers were determined by measurement of OD_{650}. All the MTb infections were done at a ratio of 1:1 (cells:bacilli).

Cell Culture

PBMCs were isolated by Ficoll-Hypaque (Pharmacia) density gradient centrifugation. Monocytes were enriched by positive selection with CD14 microbeads (STEMCELL Technologies) and then cultured at 1 × 10^6 cells per well in six-well plates in RPMI-1640 medium with 2 mM L-glutamine (BioWhittaker), supplemented with 5% heat-inactivated human AB serum (Atlanta Biologicals) and 50 ng/ml recombinant human GM-CSF (R&D Systems). After 5 days, supernatants were replaced with GM-CSF-free medium prior to experimental analysis. More than 98% of the adherent cells obtained with this technique were CD14$^+$ macrophages, as verified by flow cytometry. THP-1 cells were obtained from ATCC and cultured in RPMI-1640 medium supplemented with

10% fetal calf serum (FCS, BioWhittaker). The 293T and A549 cells were obtained from ATCC and were maintained in DMEM (BioWhittaker) supplemented with 10% FCS.

Cell Lines

Lentiviral plasmids (pLKO.1 parent vector) encoding an shRNA targeting human IFITM1–3, or a scrambled control shRNA sequence, were obtained from Dharmacon and validated in our laboratory. The pLX304-IFITM3-V5 tag plasmids, expressing IFITM3 protein and the pLX304-V5 parent vector, were obtained from the Dana Farber/Harvard Cancer Center DNA Resource Core and Addgene, respectively.

To generate *IFITM1*, *IFITM2*, and *IFITM3* expression vectors, oligoDT-primed cDNA was prepared from IFNβ-stimulated THP-1 cells and used as template for synthesis of *IFITM1*, *IFITM2*, or *IFITM3* coding regions. A GGGGS linker and flag tag were incorporated in-frame at the 3′ end of each IFITM cDNA during PCR. The *IFITM1*-Flag, *IFITM2*-Flag, and *IFITM3*-Flag sequences were cloned into MluI and NheI sites under the control of the human EF1α promoter in a pLKO.1-derived vector that also encodes a human PGK-driven puromycin resistance Pac gene.

Lentiviruses were generated by transfecting 293T cells with the plasmids above in combination with the packaging plasmid psPAX2 and the envelope plasmid pMD2.G using Effectene transfection reagent (QIAGEN). Supernatants were collected 24 and 48 hr post-transfection, clarified by centrifugation, and stored at −80°C. THP-1 cells or A549 cells were transduced with lentiviral particles in the presence of 8 μg/ml polybrene (Millipore) and spinoculation. Transduced cells were selected and expanded by treatment with 1 μg/ml puromycin or 10 μg/ml blasticidin. THP-1 cells stably transduced with lentiviruses encoding shRNAs against MyD88, IRAK1, or TRAF6 were described previously (Ranjbar et al., 2012).

qPCR

The mRNA expression levels were determined by SYBR Green-based real-time PCR (Applied Biosystems) with the following gene-specific primers: *IFITM1* (forward, 5′-ATCCTGTTACTGGTATTCGG-3′; reverse, 5′-TATAAACT GCTGTATCTAGG-3′); *IFITM2* (forward, 5′-GTTGGTCGTCCAGGCCCAGC-3′; reverse, 5′-CTGTGGGGACAGGGCGAGGA-3′); *IFITM3* (forward, 5′-GCTG ATCTTCCAGGCCTATG-3′; reverse, 5′-GATACAGGACTCGGCTCCGG-3); *IL1B* (forward, 5′-GCTGAGGAAGATGCTGGTTC-3′; reverse, 5′-TCCATATCC TGTCCCTGGAG-3′); *IL-6* (forward, 5′-AGGAGACTTGCCTGGTGAAA-3′; reverse, 5′-CAGGGGTGGTTATTGCATCT-3′); *IFNB1* (forward, 5′-GAATGG GAGGCTTGAATACTGCCT-3′; reverse, 5′-TAGCAAAGATGTTCTGGAGCATC TC-3′); *TNF* (forward, 5′-TCTTCTCGAACCCCGAGTGA-3′; reverse, 5′-CCTCT GATGGCACCACCA-3′); and cyclophilin B (*PPIB*) (forward, 5′-AGAAGAAG GGGCCCAAAG-3′; reverse, 5′-AAAGATCACCCGGCCTACA-3′).

The reaction conditions were 95°C for 10 min followed by 40 cycles of 95°C for 15 s and 60°C for 1 min. The results were normalized to cyclophilin B mRNA and expressed as relative values. Specificity of each primer set was validated by measuring the mRNA level of each *IFITM* member in THP-1 cells individually overexpressing IFITM1, 2, or 3 (Figure S3).

CFU Assay

THP-1 cells expressing the IFITMs' shRNA or control shRNA (1×10^6) were seeded in six-well plates in triplicate and infected with H37Rv. After a 3-hr incubation at 37°C, the cultures were treated with 50 μg/ml puromycin for 20 min. Cells were washed three times with PBS; cultured in 3 ml fresh RPMI plus 10% FCS for 0, 48, and 72 hr; and incubated at 37°C and 5% CO_2. Following each time point, cultures were terminated, cells were treated with lysis buffer and sonicated, and serial dilutions were prepared and inoculated in Middlebrook 7H11 agar in triplicate. Colonies were analyzed on day 25 post-infection.

Flow Cytometry

For standard cytometric analyses, cells were left uninfected or infected with MTb-mCherry for the indicated time points, after which the cultures were terminated. Cells were washed with PBS, fixed with 4% paraformaldehyde, and analyzed with a five-laser FACSAria II machine (Becton Dickinson) according to standard techniques. Results were analyzed using the FlowJo software package.

For ImageStream-based analyses, IFITM3-overexpressing and control THP-1 cells, or IFITM-KD or shRNA control THP-1 cells, were infected with H37Rv-mCherry for 24 hr and then fixed with 4% paraformaldehyde. Next, 2,500 cells per sample were acquired using an Amnis ImageStreamX Mark II machine (EMD Millipore), with simultaneous collection of bright field, fluorescence, and scatter of images on a per-cell basis. Objective numerical quantification of internalized H37Rv-mCherry was performed using IDEAS software.

Fluorescence Microscopy

A549 cells stably transduced with the IFITM3-V5 tag construct or the empty vector were seeded on a small coverslip in 12-well plates in fresh media and were infected with MTb-mCherry for 3 hr, after which the cultures were washed and fresh media were added. Cells were further incubated at 37°C for 20 hr. MTb-infected cells were fixed with 4% paraformaldehyde before they were blocked and permeabilized with buffer containing 5% normal donkey serum and 0.3% Triton X-100 in PBS for 2 hr. Cells were labeled with 1:150 rabbit anti-Rab5 or 1:100 rabbit anti-Rab7 antibody (Cell Signaling Technology) overnight in antibody dilution buffer containing 1% BSA followed by 1:500 secondary donkey anti-rabbit DyLight 649 antibody (BioLegend) for 2 hr. Cells were further labeled with mouse fluorescein isothiocyanate (FITC) anti-V5 antibody (Invitrogen) overnight, after which slides were mounted in mounting media containing DAPI. Images were captured with an Olympus (FV1000) confocal microscope and Fluoview Software 2. Analysis was performed using ImageJ software.

Staining of Acidified Compartments

THP-1 cells stably expressing IFITM3-V5 tag or empty vector were infected with H37Rv MTb for 48 hr, at which time they were incubated with LysoTracker Red DND-99 (LTRed, Life Technologies) at 50 nM for 2 hr at 37°C. Cells were washed and fixed with 4% paraformaldehyde before analysis by flow cytometry as described above.

Statistical Analysis

Where applicable, results are expressed as mean ± SEM. Comparison between two groups was performed using the unpaired Student's t test with the aid of Microsoft Excel software. A p value ≤ 0.05 was considered significant.

SUPPLEMENTAL INFORMATION

Supplemental Information includes six figures and can be found with this article online at http://dx.doi.org/10.1016/j.celrep.2015.09.048.

ACKNOWLEDGMENTS

This work was supported by grants to A.E.G. from the Annenberg Foundation, the Ragon Institute of Harvard University, the National Institute of Allergy and Infectious Diseases (NIAID, R56128154), and a gift from John Moores. S.R. was supported by a grant from the Campbell Foundation. We are grateful to Harry Leung, Michelle Ocana, Lai Ding, and Raphael Gaudin for critical assistance in performing the confocal microscopy and its analysis. We thank Sam Behar for helpful discussions and are indebted to Sabrina Hawthorne, Richard DeMarco, and Natasha Barteneva for invaluable help with IDEAS software and the Imagestream analysis. We also thank Judy Lieberman for helpful comments on the manuscript and Renate Hellmiss for the artwork.

Received: December 27, 2014
Revised: August 10, 2015
Accepted: September 17, 2015
Published: October 22, 2015

REFERENCES

Ackrill, A.M., Reid, L.E., Gilbert, C.S., Gewert, D.R., Porter, A.C., Lewin, A.R., Stark, G.R., and Kerr, I.M. (1991). Differential response of the human 6-16 and 9-27 genes to alpha and gamma interferons. Nucleic Acids Res. *19*, 591–598.

Amini-Bavil-Olyaee, S., Choi, Y.J., Lee, J.H., Shi, M., Huang, I.C., Farzan, M., and Jung, J.U. (2013). The antiviral effector IFITM3 disrupts intracellular cholesterol homeostasis to block viral entry. Cell Host Microbe *13*, 452–464.

Armstrong, J.A., and Hart, P.D. (1971). Response of cultured macrophages to Mycobacterium tuberculosis, with observations on fusion of lysosomes with phagosomes. J. Exp. Med. *134*, 713–740.

Bach, H., Papavinasasundaram, K.G., Wong, D., Hmama, Z., and Av-Gay, Y. (2008). Mycobacterium tuberculosis virulence is mediated by PtpA dephosphorylation of human vacuolar protein sorting 33B. Cell Host Microbe *3*, 316–322.

Bermudez, L.E., and Goodman, J. (1996). Mycobacterium tuberculosis invades and replicates within type II alveolar cells. Infect. Immun. *64*, 1400–1406.

Berry, M.P., Blankley, S., Graham, C.M., Bloom, C.I., and O'Garra, A. (2013). Systems approaches to studying the immune response in tuberculosis. Curr. Opin. Immunol. *25*, 579–587.

Brass, A.L., Huang, I.C., Benita, Y., John, S.P., Krishnan, M.N., Feeley, E.M., Ryan, B.J., Weyer, J.L., van der Weyden, L., Fikrig, E., et al. (2009). The IFITM proteins mediate cellular resistance to influenza A H1N1 virus, West Nile virus, and dengue virus. Cell *139*, 1243–1254.

Collins, A.C., Cai, H., Li, T., Franco, L.H., Li, X.D., Nair, V.R., Scharn, C.R., Stamm, C.E., Levine, B., Chen, Z.J., and Shiloh, M.U. (2015). Cyclic GMP-AMP Synthase Is an Innate Immune DNA Sensor for Mycobacterium tuberculosis. Cell Host Microbe *17*, 820–828.

Deguine, J., and Barton, G.M. (2014). MyD88: a central player in innate immune signaling. F1000Prime Rep. *6*, 97.

Desai, T.M., Marin, M., Chin, C.R., Savidis, G., Brass, A.L., and Melikyan, G.B. (2014). IFITM3 restricts influenza A virus entry by blocking the formation of fusion pores following virus-endosome hemifusion. PLoS Pathog. *10*, e1004048.

Dey, B., Dey, R.J., Cheung, L.S., Pokkali, S., Guo, H., Lee, J.H., and Bishai, W.R. (2015). A bacterial cyclic dinucleotide activates the cytosolic surveillance pathway and mediates innate resistance to tuberculosis. Nat. Med. *21*, 401–406.

Diamond, M.S., and Farzan, M. (2013). The broad-spectrum antiviral functions of IFIT and IFITM proteins. Nat. Rev. Immunol. *13*, 46–57.

Etna, M.P., Giacomini, E., Severa, M., and Coccia, E.M. (2014). Pro- and anti-inflammatory cytokines in tuberculosis: a two-edged sword in TB pathogenesis. Semin. Immunol. *26*, 543–551.

Everitt, A.R., Clare, S., Pertel, T., John, S.P., Wash, R.S., Smith, S.E., Chin, C.R., Feeley, E.M., Sims, J.S., Adams, D.J., et al.; GenISIS Investigators; MOSAIC Investigators (2012). IFITM3 restricts the morbidity and mortality associated with influenza. Nature *484*, 519–523.

Everitt, A.R., Clare, S., McDonald, J.U., Kane, L., Harcourt, K., Ahras, M., Lall, A., Hale, C., Rodgers, A., Young, D.B., et al. (2013). Defining the range of pathogens susceptible to Ifitm3 restriction using a knockout mouse model. PLoS ONE *8*, e80723.

Falvo, J.V., Ranjbar, S., Jasenosky, L.D., and Goldfeld, A.E. (2011). Arc of a vicious circle: pathways activated by Mycobacterium tuberculosis that target the HIV-1 long terminal repeat. Am. J. Respir. Cell Mol. Biol. *45*, 1116–1124.

Feeley, E.M., Sims, J.S., John, S.P., Chin, C.R., Pertel, T., Chen, L.M., Gaiha, G.D., Ryan, B.J., Donis, R.O., Elledge, S.J., and Brass, A.L. (2011). IFITM3 inhibits influenza A virus infection by preventing cytosolic entry. PLoS Pathog. *7*, e1002337.

Friedman, R.L., Manly, S.P., McMahon, M., Kerr, I.M., and Stark, G.R. (1984). Transcriptional and posttranscriptional regulation of interferon-induced gene expression in human cells. Cell *38*, 745–755.

Gagneux, S. (2012). Host-pathogen coevolution in human tuberculosis. Philos. Trans. R. Soc. Lond. B Biol. Sci. *367*, 850–859.

Han, J.H., Lee, S., Park, Y.S., Park, J.S., Kim, K.Y., Lim, J.S., Oh, K.S., and Yang, Y. (2011). IFITM6 expression is increased in macrophages of tumor-bearing mice. Oncol. Rep. *25*, 531–536.

Huang, I.C., Bailey, C.C., Weyer, J.L., Radoshitzky, S.R., Becker, M.M., Chiang, J.J., Brass, A.L., Ahmed, A.A., Chi, X., Dong, L., et al. (2011). Distinct patterns of IFITM-mediated restriction of filoviruses, SARS coronavirus, and influenza A virus. PLoS Pathog. *7*, e1001258.

Ishii, K., Kurita-Taniguchi, M., Aoki, M., Kimura, T., Kashiwazaki, Y., Matsumoto, M., and Seya, T. (2005). Gene-inducing program of human dendritic cells in response to BCG cell-wall skeleton (CWS), which reflects adjuvancy required for tumor immunotherapy. Immunol. Lett. *98*, 280–290.

Jia, R., Pan, Q., Ding, S., Rong, L., Liu, S.L., Geng, Y., Qiao, W., and Liang, C. (2012). The N-terminal region of IFITM3 modulates its antiviral activity by regulating IFITM3 cellular localization. J. Virol. *86*, 13697–13707.

John, S.P., Chin, C.R., Perreira, J.M., Feeley, E.M., Aker, A.M., Savidis, G., Smith, S.E., Elia, A.E., Everitt, A.R., Vora, M., et al. (2013). The CD225 domain of IFITM3 is required for both IFITM protein association and inhibition of influenza A virus and dengue virus replication. J. Virol. *87*, 7837–7852.

Kelly, J.M., Gilbert, C.S., Stark, G.R., and Kerr, I.M. (1985). Differential regulation of interferon-induced mRNAs and c-myc mRNA by alpha- and gamma-interferons. Eur. J. Biochem. *153*, 367–371.

Lewin, A.R., Reid, L.E., McMahon, M., Stark, G.R., and Kerr, I.M. (1991). Molecular analysis of a human interferon-inducible gene family. Eur. J. Biochem. *199*, 417–423.

Lin, T.Y., Chin, C.R., Everitt, A.R., Clare, S., Perreira, J.M., Savidis, G., Aker, A.M., John, S.P., Sarlah, D., Carreira, E.M., et al. (2013). Amphotericin B increases influenza A virus infection by preventing IFITM3-mediated restriction. Cell Rep. *5*, 895–908.

Lu, J., Pan, Q., Rong, L., He, W., Liu, S.L., and Liang, C. (2011). The IFITM proteins inhibit HIV-1 infection. J. Virol. *85*, 2126–2137.

Mayer-Barber, K.D., and Sher, A. (2015). Cytokine and lipid mediator networks in tuberculosis. Immunol. Rev. *264*, 264–275.

McDonough, K.A., and Kress, Y. (1995). Cytotoxicity for lung epithelial cells is a virulence-associated phenotype of Mycobacterium tuberculosis. Infect. Immun. *63*, 4802–4811.

Means, T.K., Wang, S., Lien, E., Yoshimura, A., Golenbock, D.T., and Fenton, M.J. (1999). Human toll-like receptors mediate cellular activation by Mycobacterium tuberculosis. J. Immunol. *163*, 3920–3927.

Mills, T.C., Rautanen, A., Elliott, K.S., Parks, T., Naranbhai, V., Ieven, M.M., Butler, C.C., Little, P., Verheij, T., Garrard, C.S., et al. (2014). IFITM3 and susceptibility to respiratory viral infections in the community. J. Infect. Dis. *209*, 1028–1031.

Mudhasani, R., Tran, J.P., Retterer, C., Radoshitzky, S.R., Kota, K.P., Altamura, L.A., Smith, J.M., Packard, B.Z., Kuhn, J.H., Costantino, J., et al. (2013). IFITM-2 and IFITM-3 but not IFITM-1 restrict Rift Valley fever virus. J. Virol. *87*, 8451–8464.

Nakajima, A., Ibi, D., Nagai, T., Yamada, S., Nabeshima, T., and Yamada, K. (2014). Induction of interferon-induced transmembrane protein 3 gene expression by lipopolysaccharide in astrocytes. Eur. J. Pharmacol. *745*, 166–175.

Palanisamy, G.S., DuTeau, N., Eisenach, K.D., Cave, D.M., Theus, S.A., Kreiswirth, B.N., Basaraba, R.J., and Orme, I.M. (2009). Clinical strains of Mycobacterium tuberculosis display a wide range of virulence in guinea pigs. Tuberculosis (Edinb.) *89*, 203–209.

Park, J.S., Tamayo, M.H., Gonzalez-Juarrero, M., Orme, I.M., and Ordway, D.J. (2006). Virulent clinical isolates of Mycobacterium tuberculosis grow rapidly and induce cellular necrosis but minimal apoptosis in murine macrophages. J. Leukoc. Biol. *79*, 80–86.

Ranjbar, S., Boshoff, H.I., Mulder, A., Siddiqi, N., Rubin, E.J., and Goldfeld, A.E. (2009). HIV-1 replication is differentially regulated by distinct clinical strains of Mycobacterium tuberculosis. PLoS ONE *4*, e6116.

Ranjbar, S., Jasenosky, L.D., Chow, N., and Goldfeld, A.E. (2012). Regulation of Mycobacterium tuberculosis-dependent HIV-1 transcription reveals a new role for NFAT5 in the toll-like receptor pathway. PLoS Pathog. *8*, e1002620.

Reid, L.E., Brasnett, A.H., Gilbert, C.S., Porter, A.C., Gewert, D.R., Stark, G.R., and Kerr, I.M. (1989). A single DNA response element can confer inducibility by both alpha- and gamma-interferons. Proc. Natl. Acad. Sci. USA *86*, 840–844.

Sällman Almén, M., Bringeland, N., Fredriksson, R., and Schiöth, H.B. (2012). The dispanins: a novel gene family of ancient origin that contains 14 human members. PLoS ONE *7*, e31961.

Saunders, B.M., Frank, A.A., Orme, I.M., and Cooper, A.M. (2000). Interleukin-6 induces early gamma interferon production in the infected lung but is not required for generation of specific immunity to Mycobacterium tuberculosis infection. Infect. Immun. *68*, 3322–3326.

Seok, J., Warren, H.S., Cuenca, A.G., Mindrinos, M.N., Baker, H.V., Xu, W., Richards, D.R., McDonald-Smith, G.P., Gao, H., Hennessy, L., et al.; Inflammation and Host Response to Injury, Large Scale Collaborative Research Program (2013). Genomic responses in mouse models poorly mimic human inflammatory diseases. Proc. Natl. Acad. Sci. USA *110*, 3507–3512.

Shen, C., Wu, X.R., Jiao, W.W., Sun, L., Feng, W.X., Xiao, J., Miao, Q., Liu, F., Yin, Q.Q., Zhang, C.G., et al. (2013). A functional promoter polymorphism of IFITM3 is associated with susceptibility to pediatric tuberculosis in Han Chinese population. PLoS ONE *8*, e67816.

Sillé, F.C., Martin, C., Jayaraman, P., Rothchild, A., Fortune, S., Besra, G.S., Behar, S.M., and Boes, M. (2011). Requirement for invariant chain in macrophages for Mycobacterium tuberculosis replication and CD1d antigen presentation. Infect. Immun. *79*, 3053–3063.

Smith, L.M., and May, R.C. (2013). Mechanisms of microbial escape from phagocyte killing. Biochem. Soc. Trans. *41*, 475–490.

Stanley, S.A., and Cox, J.S. (2013). Host-pathogen interactions during *Mycobacterium tuberculosis* infections. Curr. Top. Microbiol. Immunol. *374*, 211–241.

Sturgill-Koszycki, S., Schlesinger, P.H., Chakraborty, P., Haddix, P.L., Collins, H.L., Fok, A.K., Allen, R.D., Gluck, S.L., Heuser, J., and Russell, D.G. (1994). Lack of acidification in Mycobacterium phagosomes produced by exclusion of the vesicular proton-ATPase. Science *263*, 678–681.

Underhill, D.M., Ozinsky, A., Smith, K.D., and Aderem, A. (1999). Toll-like receptor-2 mediates mycobacteria-induced proinflammatory signaling in macrophages. Proc. Natl. Acad. Sci. USA *96*, 14459–14463.

Via, L.E., Tsytsykova, A.V., Rajsbaum, R., Falvo, J.V., and Goldfeld, A.E. (2012). The transcription factor NFATp plays a key role in susceptibility to TB in mice. PLoS ONE *7*, e41427.

Wassermann, R., Gulen, M.F., Sala, C., Perin, S.G., Lou, Y., Rybniker, J., Schmid-Burgk, J.L., Schmidt, T., Hornung, V., Cole, S.T., and Ablasser, A. (2015). Mycobacterium tuberculosis Differentially Activates cGAS- and Inflammasome-Dependent Intracellular Immune Responses through ESX-1. Cell Host Microbe *17*, 799–810.

Watson, R.O., Bell, S.L., MacDuff, D.A., Kimmey, J.M., Diner, E.J., Olivas, J., Vance, R.E., Stallings, C.L., Virgin, H.W., and Cox, J.S. (2015). The Cytosolic Sensor cGAS Detects Mycobacterium tuberculosis DNA to Induce Type I Interferons and Activate Autophagy. Cell Host Microbe *17*, 811–819.

Wee, Y.S., Roundy, K.M., Weis, J.J., and Weis, J.H. (2012). Interferon-inducible transmembrane proteins of the innate immune response act as membrane organizers by influencing clathrin and v-ATPase localization and function. Innate Immun. *18*, 834–845.

Weston, S., Czieso, S., White, I.J., Smith, S.E., Kellam, P., and Marsh, M. (2014). A membrane topology model for human interferon inducible transmembrane protein 1. PLoS ONE *9*, e104341.

Williams, D.E., Wu, W.L., Grotefend, C.R., Radic, V., Chung, C., Chung, Y.H., Farzan, M., and Huang, I.C. (2014). IFITM3 polymorphism rs12252-C restricts influenza A viruses. PLoS ONE *9*, e110096.

Wong, D., Bach, H., Sun, J., Hmama, Z., and Av-Gay, Y. (2011). Mycobacterium tuberculosis protein tyrosine phosphatase (PtpA) excludes host vacuolar-H+-ATPase to inhibit phagosome acidification. Proc. Natl. Acad. Sci. USA *108*, 19371–19376.

Zhang, Z., Liu, J., Li, M., Yang, H., and Zhang, C. (2012). Evolutionary dynamics of the interferon-induced transmembrane gene family in vertebrates. PLoS ONE *7*, e49265.

Zhang, Y.H., Zhao, Y., Li, N., Peng, Y.C., Giannoulatou, E., Jin, R.H., Yan, H.P., Wu, H., Liu, J.H., Liu, N., et al. (2013). Interferon-induced transmembrane protein-3 genetic variant rs12252-C is associated with severe influenza in Chinese individuals. Nat. Commun. *4*, 1418.

Zhang, Y., Makvandi-Nejad, S., Qin, L., Zhao, Y., Zhang, T., Wang, L., Repapi, E., Taylor, S., McMichael, A., Li, N., et al. (2015). Interferon-induced transmembrane protein-3 rs12252-C is associated with rapid progression of acute HIV-1 infection in Chinese MSM cohort. AIDS *29*, 889–894.